Am J Cancer Res 2015;5(11):3422-3435
www.ajcr.us /ISSN:2156-6976/ajcr0017335

Original Article

Tumor-selective anti-cancer effects of the synthetic alkyl phosphocholine analog CLR1404 in neuroblastoma

Roberta Marino[1*], Dana C Baiu[2*], Saswati Bhattacharya[2], Benjamin Titz[3], Ellen Hebron[4], Bryan D Menapace[2], Sorabh Singhal[2], Jens C Eickhoff[6], Fotis Asimakopoulos[4], Jamey P Weichert[3,5], Mario Otto[2]

[1]Department of Pathology, St. Jude Children's Research Hospital, 262 Danny Thomas Place, Memphis, TN 38105, USA; [2]Division of Pediatric Hematology, Oncology and Bone Marrow Transplant, Department of Pediatrics, University of Wisconsin-Madison School of Medicine and Public Health, 1111 Highland Avenue, Madison, WI 53705, USA; [3]Cellectar Biosciences, 3301 Agriculture Drive, Madison, WI 53716, USA; [4]Department of Medicine, University of Wisconsin-Madison 1111 Highland Avenue, Madison, WI 53705, USA; [5]Departments of Radiology and Medical Physics, University of Wisconsin-Madison School of Medicine and Public Health, 1111 Highland Avenue, Madison, WI 53705, USA; [6]Department of Biostatistics and Medical Informatics, University of Wisconsin-Madison, 600 Highland Avenue, Madison, WI 53792, USA. [*]Equal contributors.

Received October 5, 2015; Accepted October 8, 2015; Epub October 15, 2015; Published November 1, 2015

Abstract: Neuroblastoma (NB) is the most common extracranial solid tumor in children and is associated with high mortality in advanced stages. Survivors suffer from long-term treatment-related sequelae. Thus, new targeted treatment options are urgently needed. 18-(p-[^{127}I] iodophenyl) octadecyl phosphocholine (CLR1404) is a novel, broadly tumor targeted small molecule drug suitable for intravenous injection with highly selective tumor uptake. As a carrier molecule for radioactive iodine, CLR1404 is in clinical trials as cancer imaging agent and radiotherapeutic drug. Chemically, CLR1404 belongs to the anti-tumor alkyl phospholipids, a class of drugs known to have intrinsic cytotoxic effects on cancer cells. Therefore, we hypothesized that CLR1404 could be a tumor-targeted anti-cancer agent for neuroblastoma, and investigated its effect *in vitro* and *in vivo*. CLR1404 was taken up by NB cells in a highly tumor-selective manner both *in vitro* and *in vivo*, confirmed by flow cytometry and PET/CT imaging of mouse flank xenografts with ^{124}I-CLR1404, respectively. Using flow cytometry, MTT assay, Western blotting and caspase 3/7 assay, we confirm that *in vitro* treatment with CLR1404 leads to robust apoptosis and cell death in multiple NB cell lines and is associated with Akt inhibition, while sparing normal cells. Treatment with CLR1404 in doses of 10 or 30 mg/kg administered by intravenous injection once weekly for 7 weeks significantly inhibited the tumor growth rate in a mouse flank xenograft model of NB ($P<0.001$) when compared to control cohorts, without causing drug-related hematotoxicity or other noticeable adverse effects, which was determined by serial tumor volume measurements, complete blood counts, and monitoring of animal-specific health parameters. We conclude that CLR1404 warrants clinical exploration as a novel, tumor selective anticancer agent in NB and potentially other cancers.

Keywords: Neuroblastoma, CLR1404, alkyl phospholipid, alkyl phosphocholine analog, targeted therapy, Akt, pediatric cancer

Introduction

Advanced-stage neuroblastoma (NB) is a particularly difficult-to-treat childhood cancer and responsible for almost 15% of pediatric cancer mortality. The majority of patients present with metastatic disease, are classified as high-risk and have a dismal prognosis, with overall survival rates of only 40-50% despite standard multimodality therapy which includes chemotherapy, radiation, surgery, autologous stem cell transplant and immunotherapy [1]. Many survivors are stricken with long-term treatment-related sequelae, such as hearing loss, renal insufficiency or second cancers. Innovative, tumor-targeting treatment options are urgently needed to improve cure rates for this devastating pediatric cancer, ideally without additional toxicity to the already highly aggressive treatment armamentarium.

Anti-tumor alkyl phospholipids (APLs) are unique molecules which, in contrast to classical DNA-targeted chemotherapeutics, target cellu-

lar and intracellular membranes. APLs demonstrate remarkable tumor selectivity, attributed in part to selective uptake via lipid rafts, which are much more abundant in cancer cell membranes when compared to normal, healthy cells [2]. Although the anti-cancer mechanisms of APLs have not yet been fully elucidated, some of the known anti-cancer effects of APLs are interference with phosphatidylcholine biosynthesis, inhibition of lipid-mediated signal transduction pathways and membrane microdomain formation, as well as inhibition of the PI3K/Akt/mTOR signaling pathway [3]. Despite the tumor selectivity and anti-cancer properties of alkyl phospholipids, few of these compounds have entered clinical trials, largely due to the lack of intravenous formulations and limited bioavailability, as well as gastrointestinal toxicities of oral preparations [4].

18-(p-[^{127}I] iodophenyl) octadecyl phosphocholine (CLR1404) is a novel alkyl phosphocholine subtype of the anti-tumor alkyl phospholipids. During the development phase, meticulous structure-relationship studies were performed to evaluate the effect of alterations in molecular structure on tumor uptake and retention, and subsequently the herein described CLR-1404 (previously NM404) was identified as the most promising analog with best tumor uptake and retention, and most favorable toxicity profile in rodent models [5]. Radioiodinated and optically active versions of CLR1404 have demonstrated tumor selectivity in over 60 spontaneous, orthotopic and xenographic models (6). CLR1404 is highly selective for malignant tumors, formulated for intravenous administration and available in radioiodinated and optical modifications suitable for PET/CT and molecular radiotherapy. We recently reported our data on uptake and tumor retention of CLR1404 in adult cancers [6, 7]. Radioiodinated CLR1404 is currently being clinically evaluated in Phase 1 and 2 clinical imaging and radiotherapy trials in adult cancer patients. For pre-clinical applications, CLR1404 has been conjugated to various fluorescent dyes [8]. Since CLR1404 chemically belongs to the drug class of anti-tumor alkyl phospholipids, we hypothesized that non-radioactive CLR1404, albeit in much higher mass doses than needed as a carrier molecule for imaging or radiotherapy, could be a potent and potentially broadly applicable anti-cancer agent.

Here, we report our pre-clinical results investigating and confirming selective uptake, retention and anticancer effect of CLR1404 *in vitro* and *in vivo* in a rodent xenograft model of a particularly hard-to-cure pediatric malignancy, neuroblastoma. We aim to provide the rationale for further pre-clinical and clinical evaluation in neuroblastoma and potentially other cancers.

Materials and methods

Cells

Human NB cell lines were kindly provided by Dr. Andrew Davidoff, St. Jude Children's Research Hospital, Memphis, TN (NB-1691, SK-N-AS, LAN-5) and Dr. Wayne A. Warner, Children's Hospital of Los Angeles, CA (CHLA-20). Primary cultures of normal human cells at low passages (normal human skin/HUFI, and human pancreatic islet cells HI206R) were kindly provided by Dr. Victoria Browning and Dr. Luis Fernandez, respectively (University of Wisconsin-Madison). Normal cells were maintained in DMEM with essential and non-essential amino acids. Tumor cells were cultured in RPMI-1640 medium, except CHLA-20, which was cultured in IMDM. Besides 10% fetal bovine serum (FBS, Gibco-BRL, Grand Island, NY), cell growth media also contained 4 mM L-glutamine, 100 U/ml penicillin and 100 μg/ml streptomycin (Corning Cellgro, Manassas, VA). Cultured cell doubling time was calculated as (measurement time)/$\log_2$ (final cell number/initial cell number).

Mice

Animal experiments were conducted under protocols approved by the Institutional Animal Care and Use Committee of the University of Wisconsin-Madison. For heterotopic injection, 100 μl cell suspension containing 3×10^6 tumor cells (>95% viability, passage 5-25) was inoculated into subcutaneous tissue of the left flank of 6-8 week-old NSG (NOD.Cg-Prkdc^{scid} Il2rg^{tm1Wjl}/SzJ, Jackson Laboratory, Bar Harbor, ME), or nude (CrTac:NCr-*Foxn1*^{nu} Taconic, Hudson, NY) mice for imaging experiments and therapeutic experiments respectively.

Experimental CLR1404 and derivatives

18-(p-[^{127}I] iodophenyl) octadecyl phosphocholine (CLR1404) and derivatives were kindly pro-

vided by Cellectar Biosciences, Madison, WI. Analogue CLR1404 (^{127}I-CLR1404) was utilized for *in vitro* and *in vivo* assays; fluorescent CLR1501 (CLR1404-BODIPY FL) for uptake experiments and radioiodinated ^{124}I-CLR1404 was used for PET/CT imaging. For all *in vitro* assays, cells were cultured at 5×10^5 cells/ml in the presence of various concentrations of CLR1404 in medium supplemented with 2% FBS.

CLR1404 uptake

Cells (5×10^5/ml) incubated for 16-19 h with 5 μM CLR1501 and washed with 10% FBS medium for 4 hours were measured by flow cytometry (FACSCalibur, BD Biosciences) and analyzed using FlowJo 8.2 (Tree Star, Ashland, OR). Mean fluorescence intensity (MFI) per cell was corrected for cell size by normalizing for autofluorescence variations [9]. Experiments were repeated at least 3 times.

Lipid raft density

FITC-labeled Cholera toxin subunit B (Sigma-Aldrich, St. Louis, MO) was used at 5 μg for 5×10^5 cells (saturation concentration 0.1 mg/ml) to probe and quantify the lipid raft marker GM1 ganglioside by flow cytometry. The MFI values were corrected for cell size as described above. Experiments were repeated three times.

MTT assay

The assay was performed as previously described [10]. Linear growth was determined for all cells. After 20 h treatment of cells with CLR1404 in triplicate, the assay was performed according to manufacturer's instructions (Sigma-Aldrich). Absorbance was read on a microplate reader (Spectramax Plus, Molecular Devices, Sunnyvale, CA). 0.7% formaldehyde was used as control of total cell death. Live cell equivalents were determined from standard curves, and calculated as percentage from 100% cell growth of the wells with medium alone. Three repeats per cell type were performed.

Cell cycle and DNA fragmentation

After incubating cells at 5×10^5 cells/ml with CLR1404 for 24 hours, cells and cellular fragments were fixed in 70% ethanol for 24 h at 4°C. Cellular DNA was stained as previously described [11]. Samples saturated in 0.1 mg/ml propidium iodide (Sigma Aldrich) were measured by flow cytometry on a FACS Calibur (BD, San Jose, CA) using a FL2 doublet-discrimination module on a linear scale. The cell cycle was analyzed with FlowJo 8.2 using the Dean-Jett Fox Model and the Watson Pragmatic Model as guides. The sub-G1 (hypodiploid) population of cell fragments was evaluated as percentage of events of the total population of propidium iodide positive non-aggregated events. As positive control, staurosporine at 1 μM was used. The experiments were repeated 3 times or more for SK-N-AS and HUFI, 4 times for CHLA-20 and LAN-5, and 8 times for NB-1691.

Western blotting

After treatment of cells at a density of 10^6 cells/ml with various concentrations of CLR1404 for 19 h, cells were detached; protein lysates were prepared in Laemmli buffer and loaded at a concentration equivalent to 10^5 cells per lane on 10% acrylamide gels. Proteins were transferred at 105 volts for 40 minutes on BioRad Mini PROTEAN Tetra Cell systems. Blots were incubated overnight in 5% w/v BSA 0.1% Tween-20 tris-borate-saline buffer with anti-Phospho-Akt (CS4058), anti-pan Akt (CS2920) and corresponding HRP-labeled secondary antibodies, and lastly probed with anti-GAPDH-HRP (all Cell Signaling, Danvers, MA). HRP was developed with ECL 2 Western Blotting Substrate (Pierce, Rockford, IL or GE Amersham, Pittsburgh, PA). Experiments were repeated three times.

Caspase-3 and caspase-7 activity assay

Caspase-Glo 3/7 Luminescent Assay (Promega, Fitchburg, WI) was used according to the manufacturer's instructions. In brief, NB cell lines were seeded into 96-well plates at 2×10^4 cells per well in triplicate and CLR1404 was added to attain concentrations of 2.5 μM, 5 μM, 10 μM 15 μM and 20 μM. 1 μM Staurosporine (Sigma-Aldrich) served as positive control [12]. Results were detected on a luminometer (Bio-Tek, Winooski, VT). The experiments were repeated twice.

In vivo PET-CT image data acquisition, processing and analysis

Once xenograft tumors measured a minimum of about 7×7 mm (corresponding to a volume of about 180 mm^3), mice received 150 μCi of ^{124}I-

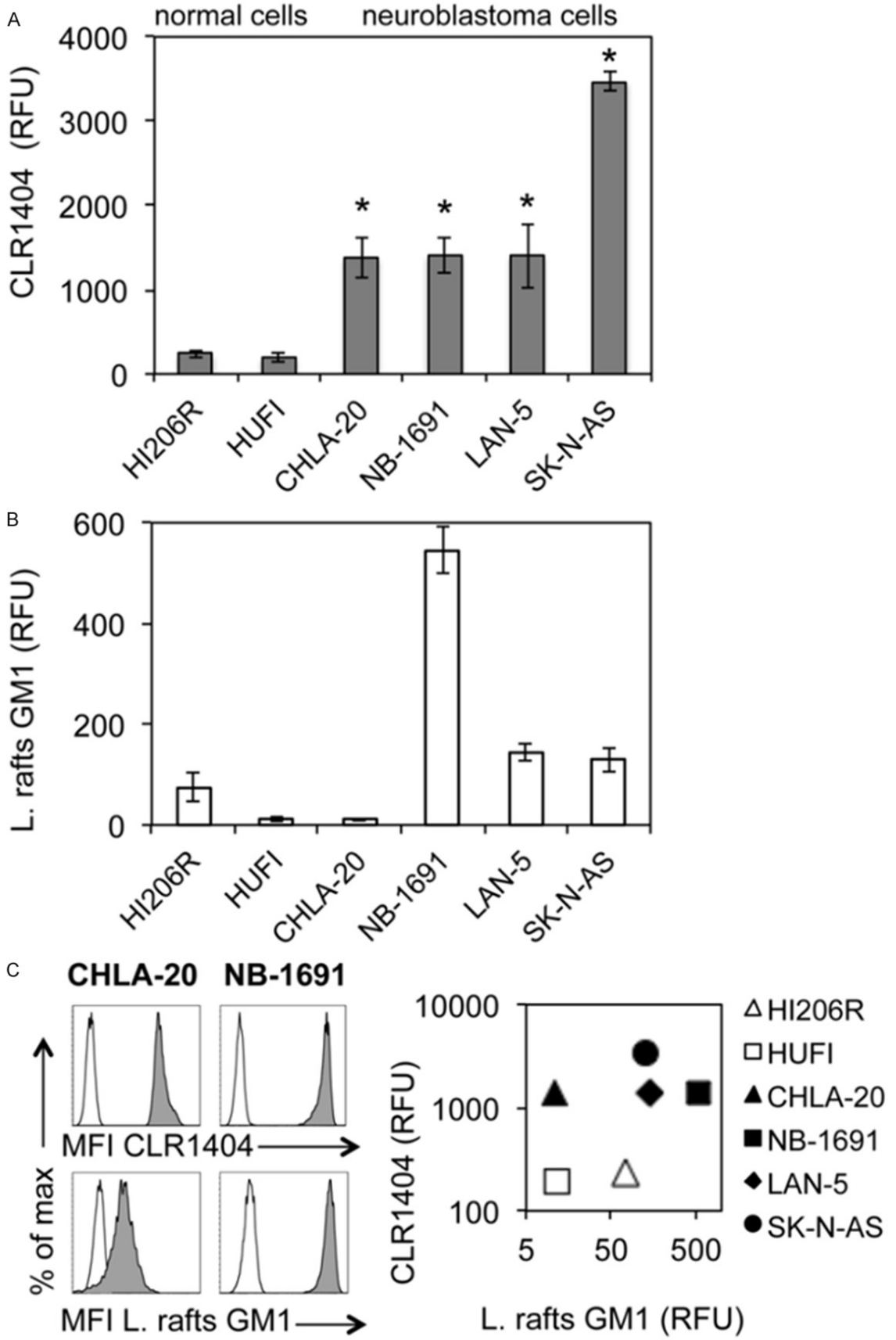
A
normal cells
neuroblastoma cells
CLR1404 (RFU)
4000
3000
2000
1000
0
*
HI206R
HUFI
CHLA-20
NB-1691
LAN-5
SK-N-AS
B
L. rafts GM1 (RFU)
600
400
200
0
C
CHLA-20
NB-1691
MFI CLR1404
% of max
MFI L. rafts GM1
CLR1404 (RFU)
10000
1000
100
5
50
500
L. rafts GM1 (RFU)
HI206R
HUFI
CHLA-20
NB-1691
LAN-5
SK-N-AS

Figure 1. Neuroblastoma cells sequester CLR1404 at higher levels than normal cells. A. Flow cytometry of the uptake of CLR1404 fluorescent analog by normal and tumor cells. Averages ± standard error (SE) from three to five repeats per cell type. *P<0.05 tumor cells versus either of the normal cells. B. Flow cytometry of the density of GM1 lipid rafts marker measured by binding of fluorescent cholera toxin subunit B to cells. Averages ± SE from three repeats per cell type. C. Absence of correlation between CLR1404 uptake and lipid raft density shown in representative histograms for two neuroblastoma cell lines (tinted histogram for fluorescence; clear for cell autofluorescence) and correlation plot (R^2<0.1). Symbols show average values for cell type. MFI: mean fluorescence intensity per cell; RFU: relative fluorescence units of MFI per cell corrected for cell size.

CLR1404 via tail-vein injection. After allowing for an uptake period of up to 96 hours [13] PET/CT image data were acquired under anesthesia on an Inveon micro-PET/CT scanner (Siemens, Knoxville, TN) in 3D acquisition mode. Static PET data acquisition was terminated after reaching a minimum of 40 million collected counts. PET images were reconstructed in 3D mode using the ordered-subset expectation maximization (OSEM3D) maximum *a posteriori* (MAP) algorithm (2 iterations, 18 subsets, and beta smoothing factor =0) with a resulting voxel size of 0.861×0.861×0.796 mm^3. PET images were imported into Amira (FEI, SAS) for visualization and further analysis. Regions of interest (ROI) were segmented for the tumors and muscle tissue (thigh muscle contralateral to the site of inoculation) based on axial slices of the CT data. Mean PET tracer uptake values and standard deviation of the CT-based ROIs were extracted using the *Material Statistics* module. For each subject, tumor-to-muscle-ratios (TMR) were calculated by normalizing the tumor ROI uptake values to the mean uptake value of the muscle ROI.

Therapeutic CLR1404 xenograft experiments

NB-1691 subcutaneous flank xenografts were induced in nude mice (see above). Tumors were measured twice weekly with calipers. The tumor volume was calculated using the following formula ($width^2 \times length \times \pi)/6$ [14]. When tumors reached approximately 50 mm^3, mice were randomly assigned to receive either CLR1404 at 10 mg/kg (n=8), CLR1404 at 30 mg/kg (n=9), or excipient solution alone (n=7) once weekly by intravenous injection, for 7 weeks. The experiment was performed twice. As controls, cohorts of non-tumor bearing nude mice were injected (lateral tail vein) weekly with 10 (n=8) or 30 mg/kg (n=9) CLR1404, or excipient solution (n=8) for 6 weeks. To determine hematotoxicity, peripheral blood samples were collected at four time points (0, 3, 5 and 7 weeks) by temporal vein puncture and evaluated for RBC count, hemoglobin concentration, and leucocyte differential analysis (lymphocytes, monocytes, granulocytes) on a VETScan HM2 (Abaxis, Union City, CA). Body weight was documented.

Statistical analysis

Analysis of variance (ANOVA) was conducted to compare lipid raft density, caspase-3, and caspase-7 activity between experimental conditions. The unpaired t-test method was used to analyze CLR1404 uptake after flow cytometry. The results were displayed in graphical format using bar plots with the corresponding standard error bars. The association between DNA fragmentation and NB culture cell doubling time was evaluated using linear regression analysis. Tumor growth from CLR1404 xenograft experiments was analyzed and compared between experimental conditions using linear mixed effects model with animal specific random effects and the log-transformed tumor volume as the outcome measure [15]. All *p*-values were two-sided and P<0.05 was used to define statistical significance. Statistical analysis was conducted using GraphPad (LaJolla, CA) and SAS software (SAS Institute Inc., Cary, NC).

Results

CLR1404 is selectively incorporated and retained by NB cell lines

All neuroblastoma tumor cell lines demonstrated statistically significant (P<0.05) CLR1404 uptake when compared to primary cells (HUFI, HI206R), ranging from 6.8 fold (CHLA-20) to 13.5 fold (SK-N-AS) difference (**Figure 1**). Affinity of CLR1404 for lipid rafts was proposed as a mechanism for selective uptake in cancer cells [6]. Despite the fact that higher levels of lipid rafts were identified on the surface of most NB cells when compared to normal cells (**Figure 1B**), no linear correlation could be established between the average lipid raft density and levels of uptake between cell lines (**Figure 1C**), suggesting additional mechanisms contributing to the high selectivity of CLR1404 for NB cells.

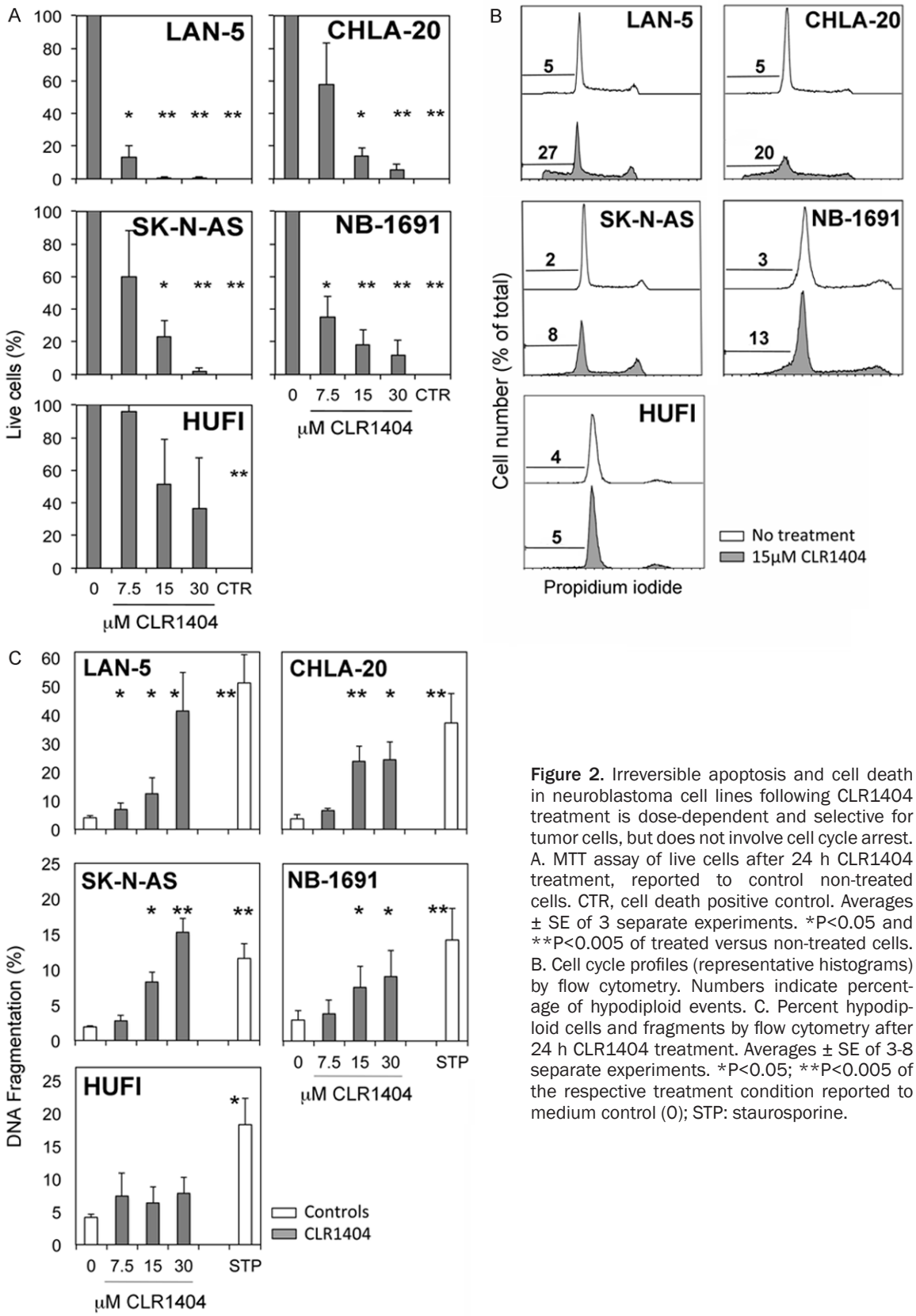

Figure 2. Irreversible apoptosis and cell death in neuroblastoma cell lines following CLR1404 treatment is dose-dependent and selective for tumor cells, but does not involve cell cycle arrest. A. MTT assay of live cells after 24 h CLR1404 treatment, reported to control non-treated cells. CTR, cell death positive control. Averages ± SE of 3 separate experiments. *P<0.05 and **P<0.005 of treated versus non-treated cells. B. Cell cycle profiles (representative histograms) by flow cytometry. Numbers indicate percentage of hypodiploid events. C. Percent hypodiploid cells and fragments by flow cytometry after 24 h CLR1404 treatment. Averages ± SE of 3-8 separate experiments. *P<0.05; **P<0.005 of the respective treatment condition reported to medium control (0); STP: staurosporine.

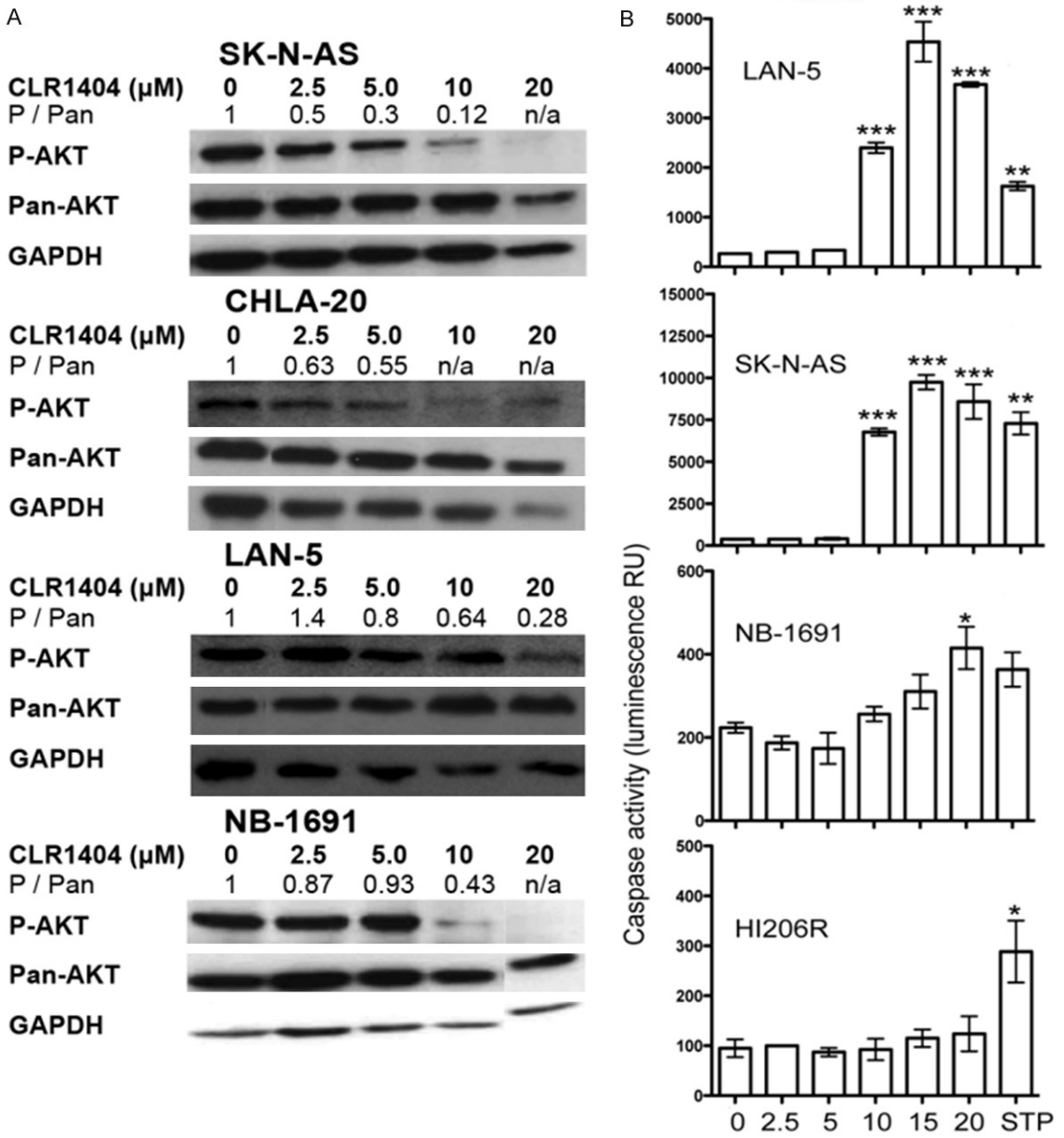

Figure 3. CLR1404 inhibits Akt phosphorylation and activates caspases 3 and 7 in neuroblastoma. A. Western blot of phosphorylated Akt (P-AKT), total Akt (T-AKT) and GAPDH in neuroblastoma cell lines, and calculated densitometric ratio P-AKT/T-AKT. Representative of 3 repeats per cell line. B. Caspase 3 and 7 activity using Caspase-Glo fluorescent substrate in neuroblastoma and normal cells. Means and 95% confidence intervals of two independent experiments are shown. *P<0.05, **P<0.01 and ***P<0.001 of treated versus non-treated cells.

CLR1404 induces cell death in NB cell lines

CLR1404 treatment in concentrations of 15 μM and above led to significantly lower tumor cell viability at 24 h (**Figure 2A**) in all tumor cell lines, when compared with no treatment or normal cell controls. In contrast, primary cell cultures indicated statistically non-significant cell death or cell growth inhibition after treatment with CLR1404 at all tested concentrations.

CLR1404 does not induce cell cycle arrest

We next investigated whether CLR1404 has an influence on the cell cycle in NB cells. Treatment of NB cells with various concentrations of CLR1404 for 24 h induced no cell cycle arrest and no other statistically significant changes (illustrated for 15 μM CLR1404 in **Figure 2B**). A decrease in the number of cells in G0/G1 phase occurred in all NB cell lines starting with 7.5 μM

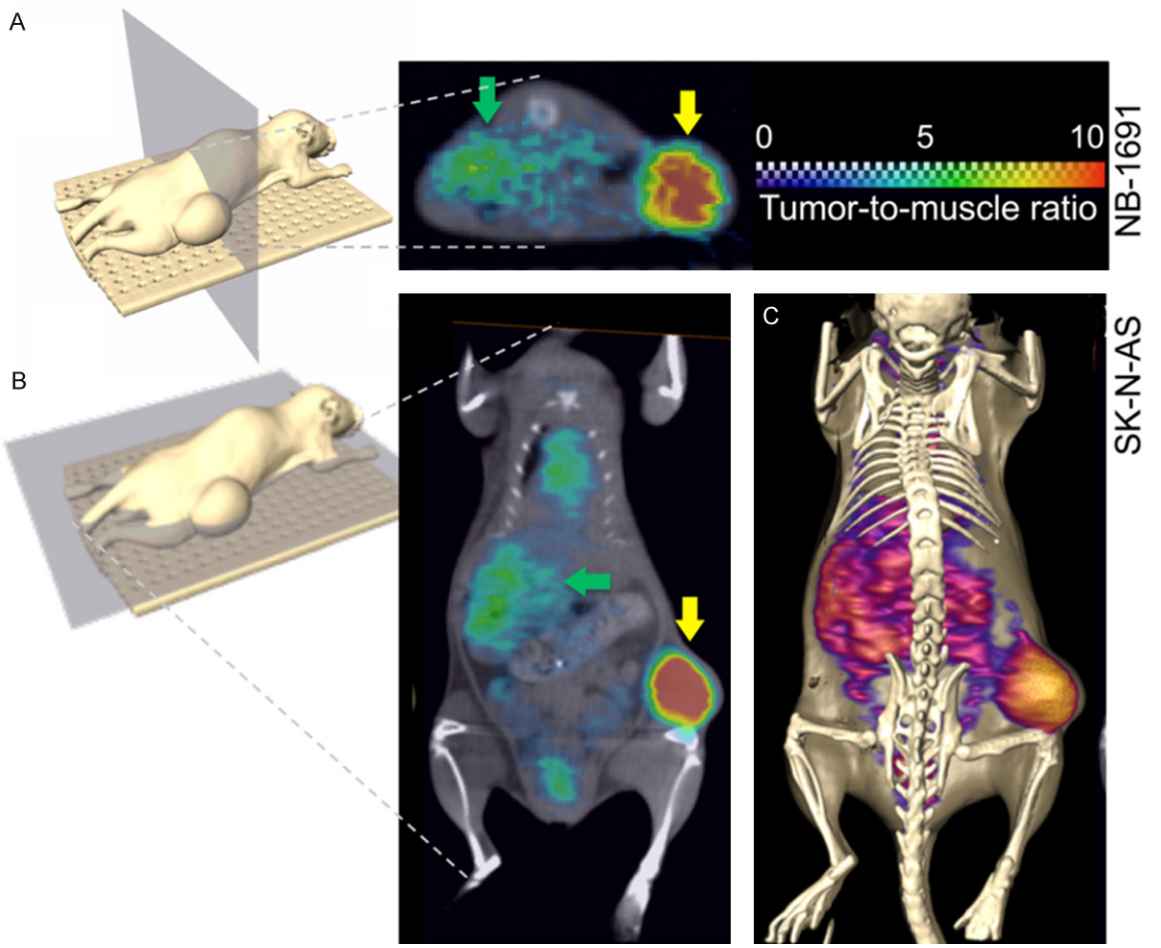

Figure 4. Axial and coronal PET/CT orthoslices illustrating the tumor uptake of ^{124}I-CLR1404 at 96 hrs post-injection. (A) Axial PET/CT orthoslice (section through CT data set with corresponding PET data 'color-washed' in) showing preferential tumor uptake (yellow arrow) and blood pool activity in the liver (green arrow) in a NB-1691 xenograft. (B) Coronal section through a PET/CT data set acquired in a SK-N-AS xenograft model illustrating ^{124}I-CLR1404 uptake levels in tumor (yellow arrow), blood pool activity in liver (green arrow), heart, and testes. (C) Identical data set shown in (B), but visualized as a CT isosurface with PET data shown as a Voltex surface.

CLR1404 (average 8% decrease, range 2-20%), but not in the normal cell controls. This decrease suggests that CLR1404 allows the G1 cells to progress through interphase beyond the G0 and G1/S checkpoints, but slows their progression through interphase and mitosis. These data suggest that the observed profound tumoricidal effect of CLR1404 on NB cells might affect cells in any phase of the cell cycle.

CLR1404 induces irreversible apoptosis by DNA fragmentation in NB cell lines

CLR1404 treatment at concentrations above 7.5 μM significantly increased the number of hypodiploid cells or DNA-containing cellular fragments in all NB cells (**Figure 2B**, **2C**), indicating DNA fragmentation. DNA fragmentation is a hallmark of the major and irreversible processes occurring in late phases of apoptosis [16], which would drive cells further towards secondary necrosis [11]. The effect of CLR1404 on DNA fragmentation was dose-dependent and not detected in primary cultures of normal skin fibroblasts, supporting the selectivity of the CLR1404 activity on tumor cells. The extent of DNA fragmentation inversely correlated with the NB culture cell doubling time (R^2=0.8), in such that the more rapidly dividing cells (CHLA-20, LAN-5) were more susceptible to DNA fragmentation after CLR1404 treatment.

CLR1404 treatment leads to inhibition of Akt phosphorylation and apoptosis signaling in a dose dependent fashion in NB cells

In many cancers, including NB, the serine/threonine protein kinase Akt is constitutively phos-

Table 1. ^{124}I-CLR1404 PET/CT image analysis

Xenograft	Mean TMR ± SD	n
LAN-5	4.10 ± 1.09	5
SK-N-AS	2.51 ± 1.31	3
NB-1691	5.29 ± 1.57	2
CHLA-20	5.79	1

TMR: Tumor-to-Muscle ratio; SD: Standard deviation; n: Number of repeats. Tumor-to-Muscle Ratios of ^{124}I-CLR1404 uptake in mice bearing flank xenografts of four human neuroblastoma cell lines.

phorylated (activated) and leads to the abrogation of pro-apoptotic signaling [17]. Several anti-tumor APLs have shown to be inhibitors of Akt [3]. Since phospholipid ethers such as CLR1404 are structurally related to APLs, we tested whether CLR1404 treatment has an effect on the expression and phosphorylation of Akt in NB1691, SK-N-AS, CHLA-20 and LAN-5 NB cells by western blotting (**Figure 3A**). CLR1404 treatment led to significant inhibition of Akt phosphorylation in all tested NB cell lines in concentrations of 10 μM and above. Inhibition of overexpressed Akt leads in many malignant cells to cleavage and activation of caspases, important mediators of apoptosis [17]. In alignment with this concept, CLR1404-treated NB cells showed a dose-dependent increase in caspase-3/7 activity in all tested NB lines in concentrations of 10 μM and above (**Figure 3B**) that was comparable or even higher than observed with the pan-protein kinase inhibitor staurosporine. CLR1404 did not elicit any significant caspase activity in normal HI206R, as the negligible drug uptake seen in previous experiments had suggested.

In vivo tumor retention of ^{124}I-CLR1404

To evaluate *in vivo* tumor selectivity and retention of CLR1404, radio-iodinated ^{124}I-CLR1404 was injected intravenously into NSG mice carrying flank xenografts of NB. All four NB cell lines used for xenograft development showed significant uptake of ^{124}I-CLR1404-PET. Representative images with NB-1691 and SK-N-AS are shown in **Figure 4**. ^{124}I-CLR1404 was tumor selective in all tested cell lines with mean TMRs (tumor-to muscle ratios) ranging from 2.51 to 5.79 and maximum TMR exceeding values of 10 (**Table 1**).

CLR1404 significantly slows tumor growth rate in a flank xenograft mouse model of NB

Next, we tested the effect of the non-radioactive, ^{127}I-CLR1404 on tumor growth rate as single therapeutic agent in a flank xenograft mouse model using a linear mixed effects model with animal specific random effects and the log-transformed tumor volume as the outcome measure. Both 10 mg/kg and 30 mg/kg CLR1404 given weekly by intravenous injection for 7 weeks significantly decreased the growth rate of the flank tumors (**Figure 5A**) when compared to the control group that received excipient only ($P<0.001$). There was no statistically significant difference in inhibition of tumor growth between the two treatment arms. Control mice demonstrated progressive tumor growth. Three mice in the 10 mg/kg CLR1404 group and one mouse in the 30 mg/kg CLR1404 group exhibited initial tumor growth, but the xenografts regressed and finally disappeared completely leading to a cure over the course of the treatment.

CLR1404 treatment is not hematotoxic in athymic nude mice and does not cause weight loss

Some APLs have shown to induce hemolysis, specifically when used intravenously [18]. Additionally, we were interested in assessing potential myelosuppression as this would to some extent influence the utility of CLR1404 in the clinical setting. After 6 weeks of treatment with either 10 or 30 mg/kg CLR1404, total white blood cell counts were within physiological limits (**Figure 5B**) [19]. A statistically non-significant decrease in mean hemoglobin concentration (1 g/dL after 6 weeks) and RBC count (1×10^{12}/L) was noted over time in all cohorts when compared to baseline counts, possibly reflecting the mild blood loss due to repeat venipuncture or variability due to the small number of mice per cohort. No significant differences in leukocyte differential counts were detected (not shown). The 6-week treatment did not cause weight loss in any of the mice (**Figure 5B**).

Discussion

We report here our studies investigating the novel, clinical-grade alkyl phospholipid CLR-

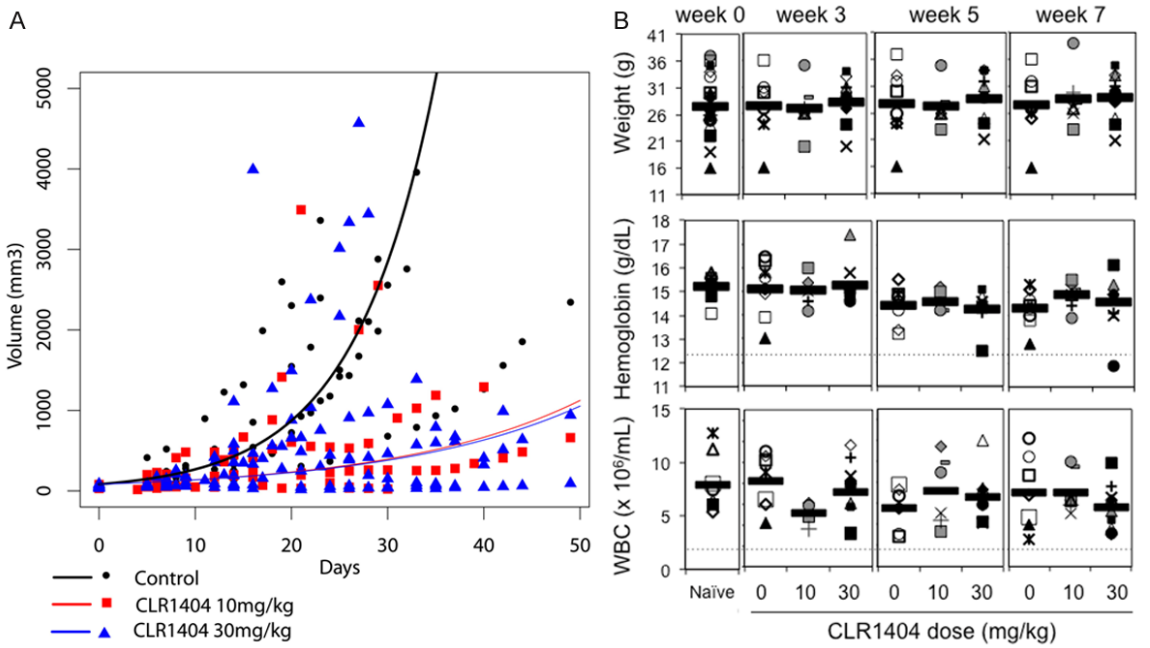

Figure 5. CLR1404 slows the growth rate of neuroblastoma xenograft tumors, but does not cause myelotoxicity or weight loss. A. Tumor volumes (symbols) and mixed effects model tumor growth rate (lines) in an NB-1691 xenograft model in nude mice treated weekly with CLR1404. Control group (excipient, black line and symbols) n=7; CLR1404 10 mg/kg (red line and symbols) group n=8; CLR1404 30 mg/kg group (blue line and symbols) n=9 mice. Both treatment regimens led to significant reduction of tumor growth rate compared to the control ($P<0.001$). B. Weight, hemoglobin, and white blood cell counts (WBC) in healthy nude mice treated weekly with CLR1404. Naïve group (not injected) n=8; control group (excipient) n=8; 10 mg/kg group n=8; 30 mg/kg group n=9 mice. Each symbol is the value for one mouse. Bar shows average per group. Dotted lines indicate lowest normal limits.

1404 as a tumor selective anti-cancer agent for the treatment of NB.

Using a fluorescent variant, CLR1404 uptake was assessed by flow cytometry in a variety of well-established NB cell lines of primary and metastatic origin. All tested NB cell lines demonstrated enhanced uptake and retention (**Figure 1A**), and indicated a 6 to 14 fold uptake enhancement in tumor vs. control cells. Incubation time and content of FBS in culture media were selected based on previous studies in numerous non-pediatric tumor cell lines showing a maximum *in vitro* uptake of CLR1404 in 5 μM concentration in 24 hours, in the presence of 2% FBS [6]. The *in vitro* cell uptake in the presence of 10% FBS takes longer, which may suggest that only free, albumin-unbound CLR1404 is readily taken up by tumor cells [6]. Uptake and retention were variable between cell lines and also showed some inter-experimental variability (**Figure 1**). It was recently reported that anti-cancer APL uptake seems to be dependent on APL type, lipid raft content, cell metabolic energy status and cancer cell type [2]. We have previously demonstrated [6] that uptake of CLR1404 in the adult prostate cancer cell line PC-3 at least partially is due to interaction with lipid rafts, as treatment with filipin III, a lipid raft disruptor, caused 50-60% less uptake when compared to controls. We determined the density of lipid rafts on NB cell lines by flow cytometry (**Figure 1B**). Our data did not suggest a correlation between raft density and CLR1404 uptake in NB cell lines (**Figure 1C**). Lipid rafts contain important signaling and transport molecules [20]. It is possible that in NB, the composition of the lipid rafts plays a greater role in CLR1404 uptake than raft quantity, or other uptake mechanisms such as energy-dependent flippases or APL translocases [21, 22] are more prominently involved in this context. Whether this observation could have clinical implications is unclear, since we did not observe a trend suggesting that uptake correlates with biological effects such as caspase activity (see **Figure 3B**).

Next, we investigated the anti-tumor, cytotoxic effects of CLR1404 in a variety of neuroblastoma lines and compared to potential effects on normal cells. CLR1404 treatment dose-dependently decreased tumor cell viability (**Figure 2A**) and led to robust and irreversible apoptosis as demonstrated by a significant percentage of DNA fragmentation in four different NB cell lines, without indication that CLR1404 has an effect on cell cycling (**Figure 2B**, **2C**). The amount of uptake of CLR1404 did not strictly correlate with the degree of apoptosis or cell death induced by CLR1404. Likely this reflects variances in cell signaling profiles of the different cell lines, as indicated by the effect of a control pan-kinase inhibitor, staurosporine. Inhibition of the anti-apoptotic PI3K/mTOR/Akt pathway has been well described as a hallmark anti-tumor mechanism mediated by APLs. In particular, the serine/threonine kinase Akt, downstream of PI3K, is a key regulator of cancer cell survival mechanisms [17, 23], and is one of the best characterized targets of APLs [3]. CLR1404 treatment led dose-dependently to inhibition of Akt phosphorylation in neuroblastoma cells in concentrations above 5 μM (**Figure 3A**) and important activation of the downstream effector caspases 3 and 7 (**Figure 3B**). We did not investigate whether inhibition of Akt phosphorylation was a direct effect of the drug on Akt itself or occurred due to indirect effects mediated by other cell signaling pathways. However, the observation is noteworthy, since activation of Akt has been reported in NB, is associated with poor prognosis [24, 25] and consequently, considered an attractive target for NB therapy [26-28]. APLs have shown several other anticancer effects that may lead to Akt-independent apoptosis, such as triggering the stress-activated protein kinase, c-Jun N-terminal kinase SAPK/JNK or other well-described apoptosis pathways which bypass Akt and could have contributed to our findings [3, 29, 30]. Regardless of the potential underlying mechanisms, all tested NB cell lines showed significant apoptosis and cell death after exposure to CLR1404, while primary cells were not affected, an important *in vitro* result which prompted us to proceed with animal experiments.

In vivo tumor uptake of CLR1404 was confirmed in mouse flank xenograft models using CT/positron-emission tomography (PET) imaging with ^{124}I-CLR1404, a radioactive isostere of CLR1404 currently in clinical trials for PET/CT imaging in adult malignancies. All tested NB xenografts were highly PET/CT avid and incorporated ^{124}I-CLR1404, with high tumor specificity (**Figure 4**; **Table 1**). While our experiments were meant as a tool to demonstrate *in vivo* tumor uptake and not powered or designed to provide data aimed at dosimetry, our results are in line with more extensive data previously published by us in adult malignancies, both in pre-clinical and clinical studies [6, 7] and suggest that ^{124}I-CLR1404 could have a potential role as an imaging agent in NB. This would be particularly interesting for NB tumors that are not avid for the clinically used scintigraphy tumor detection scan with ^{123}I-metaiodobenzylguanidine (MIBG). Separately, a recent study has suggested superiority of ^{18}F-fluorodeoxyglucose positron emission tomography (^{18}F-FDG PET/CT) compared to ^{123}I-MIBG in regards to sensitivity to detect neuroblastoma in patients [31]. Given the uptake mechanisms of ^{124}CLR1404 and its selectivity for malignant tissue that differ significantly from both ^{18}F-FDG and ^{123}I-MIBG, dedicated and comparative studies will be necessary to determine the utility of ^{124}I-CLR1404 in this particular context.

Next, we tested whether our *in vitro* detected anticancer effects of CLR1404 could be reproduced in a flank xenograft model of NB. The therapeutic regimen was selected based on pre-clinical toxicology studies of CLR1404 in rats and cynomolgus monkeys which had shown non-toxicity (based on mortality, clinical signs, body weights, food consumption, ophthalmic examinations, and clinical and anatomic pathology) at weekly injections of 10 mg/kg in rats and 4 mg/kg in non-human primates [32], and our own observations in mouse pilot experiments which suggested non-toxicity at weekly doses of 10 mg/kg or 30 mg/kg. Our data (**Figure 5A**) show a significant reduction in tumor growth rate in both treatment cohorts (10 mg/kg or 30 mg/kg) when compared to the control cohort that received excipient solution only ($P<0.001$). No statistical difference was observed between the two treatment cohorts ($P=0.988$) suggesting that the half maximal effective concentration (EC_{50}) of CLR1404 has been reached at or is below 10 mg/kg in our treatment model. Three mice in the 10 mg/kg/week cohort and one mouse in the 30 mg/kg/

week cohort exhibited initial tumor growth, but the xenografts regressed and finally disappeared completely leading to a cure over the course of the treatment, however without reaching statistical significance, perhaps due to the number of animals per cohort. Thiele et al. [26] recently described the anticancer effects of the oral APL perifosine in a mouse NB xenograft model. Perifosine (24 mg/kg) was administered daily orally by gavage for up to 32 days. Single agent perifosine treatment led to significantly reduced tumor burden at this dose level. The therapeutic index however was narrow, with lower doses (10 mg/kg, 15 mg/kg) not showing any therapeutic effect, and 36 mg/kg demonstrating severe gastrointestinal toxicity. Gastrointestinal, dose-limiting toxicity (DLT) has been described with oral and intravenously administered APLs, including perifosine, in pre-clinical as well as clinical trials [4], likely restricting their potency. Perifosine has been evaluated in a phase I study using up to 75 mg/m^2/day in nine pediatric patients with advanced solid malignancies, exhibiting a similar toxicity profile as described in the adult population [33]. In contrast, in our experiments, no weight loss was observed with the once weekly intravenous CLR1404 treatment (**Figure 5B**), neither were any other signs of impaired health, such as rough fur, hunched posture, or decreased food or water intake, leading us to conclude that CLR1404 was well tolerated in our pre-clinical mouse model at the doses tested.

Hematotoxicity, in particular hemolysis, has been a concern with some intravenous APLs [34, 35]. For instance, miltefosine demonstrated very limited oral anti-tumor activity and high hemolytic potential when given intravenously, which led to the cessation of its development as an anticancer agent [36, 37]. We therefore evaluated whether treatment of non-tumor bearing mice with our CLR1404 treatment regimen would influence hematologic parameters. No significant changes in hemoglobin concentration or total leukocyte count (**Figure 5B**) or differential leukocyte counts (granulocytes, lymphocytes, monocytes, data not shown) were observed between the cohorts over a treatment period of 6 weeks.

In summary, CLR1404 is unique amongst APLs in that this novel, clinical-grade and broadly tumor-selective molecule is extremely versatile, available in an intravenous formulation and well tolerated in *in vivo* experiments. In alignment with existing, extensive pre-clinical toxicity data in rodents and cynomolgus monkeys, CLR1404 injection did not cause hematotoxic or gastrointestinal side-effects in our pre-clinical animal models, in which we injected repetitive doses which equal approximately 100-fold the mass dose of CLR1404 per dose administered as a carrier substance of radioactive iodine for imaging (iodine-124) or for molecular radiotherapy (iodine-131) in clinical trials. Our study demonstrated that CLR1404 has potent anti-cancer effects on NB *in vitro* and *in vivo*.

We conclude that CLR1404 has the potential to become a tumor-selective anti-cancer agent in neuroblastoma and warrants clinical exploration. Future studies should investigate CLR-1404 either as single agent or in combination with chemotherapy or other therapeutic modalities in pediatric and adult malignancies.

Acknowledgements

This work was supported by a Young Investigator Award to M.O. by Alex's Lemonade Stand Foundation for Childhood Cancer Research. This work was supported in part by NIH/NCI P30 CA014520 and P30 CA014520-39 (UWCCC Comprehensive Cancer Center). We thank Cellectar, Inc., Madison, WI for providing CLR1404 and derivatives for this study and Mohammed Farhoud, M.S., for help in PET/CT image acquisition.

Disclosure of conflict of interest

Jamey P. Weichert is the founder of Cellectar Biosciences which holds the licensing rights to all phospholipid ether analogs presented here. *Benjamin Titz* is an employee of Cellectar Biosciences. No other author has potential conflicts of interest to declare.

Address correspondence to: Dr. Mario Otto, Department of Pediatrics, University of Wisconsin School of Medicine and Public Health, 1111 Highland Avenue, 4153 WIMR, Madison, WI 53705, USA. Tel: 608-265-9645; Fax: 608-265-9721; E-mail: motto@pediatrics.wisc.edu

References

[1] Maris JM. Recent advances in neuroblastoma. N Engl J Med 2010; 362: 2202-2211.
[2] Vink SR, van der Luit AH, Klarenbeek JB, Verheij M and van Blitterswijk WJ. Lipid rafts and

metabolic energy differentially determine uptake of anti-cancer alkylphospholipids in lymphoma versus carcinoma cells. Biochem Pharmacol 2007; 74: 1456-1465.
[3] van Blitterswijk WJ and Verheij M. Anticancer mechanisms and clinical application of alkylphospholipids. Biochim Biophys Acta 2013; 1831: 663-674.
[4] Vink SR, van Blitterswijk WJ, Schellens JH and Verheij M. Rationale and clinical application of alkylphospholipid analogues in combination with radiotherapy. Cancer Treat Rev 2007; 33: 191-202.
[5] Pinchuk AN, Rampy MA, Longino MA, Skinner RW, Gross MD, Weichert JP and Counsell RE. Synthesis and structure-activity relationship effects on the tumor avidity of radioiodinated phospholipid ether analogues. J Med Chem 2006; 49: 2155-2165.
[6] Weichert JP, Clark PA, Kandela IK, Vaccaro AM, Clarke W, Longino MA, Pinchuk AN, Farhoud M, Swanson KI, Floberg JM, Grudzinski J, Titz B, Traynor AM, Chen HE, Hall LT, Pazoles CJ, Pickhardt PJ and Kuo JS. Alkylphosphocholine analogs for broad-spectrum cancer imaging and therapy. Sci Transl Med 2014; 6: 240ra75.
[7] Grudzinski JJ, Titz B, Kozak K, Clarke W, Allen E, Trembath L, Stabin M, Marshall J, Cho SY, Wong TZ, Mortimer J and Weichert JP. A phase 1 study of 131I-CLR1404 in patients with relapsed or refractory advanced solid tumors: dosimetry, biodistribution, pharmacokinetics, and safety. PLoS One 2014; 9: e111652.
[8] Deming DA, Maher ME, Leystra AA, Grudzinski JP, Clipson L, Albrecht DM, Washington MK, Matkowskyj KA, Hall LT, Lubner SJ, Weichert JP and Halberg RB. Phospholipid ether analogs for the detection of colorectal tumors. PLoS One 2014; 9: e109668.
[9] Tzur A, Moore JK, Jorgensen P, Shapiro HM and Kirschner MW. Optimizing optical flow cytometry for cell volume-based sorting and analysis. PLoS One 2011; 6: e16053.
[10] Sylvester PW. Optimization of the tetrazolium dye (MTT) colorimetric assay for cellular growth and viability. Methods Mol Biol 2011; 716: 157-168.
[11] Krysko DV, Vanden Berghe T, Parthoens E, D'Herde K and Vandenabeele P. Methods for distinguishing apoptotic from necrotic cells and measuring their clearance. Methods Enzymol 2008; 442: 307-341.
[12] Zhang XD, Gillespie SK and Hersey P. Staurosporine induces apoptosis of melanoma by both caspase-dependent and -independent apoptotic pathways. Mol Cancer Ther 2004; 3: 187-197.
[13] Grudzinski JJ, Floberg JM, Mudd SR, Jeffery JJ, Peterson ET, Nomura A, Burnette RR, Tome WA, Weichert JP and Jeraj R. Application of a whole-body pharmacokinetic model for targeted radionuclide therapy to NM404 and FLT. Phys Med Biol 2012; 57: 1641-1657.
[14] Tomayko MM and Reynolds CP. Determination of subcutaneous tumor size in athymic (nude) mice. Cancer Chemother Pharmacol 1989; 24: 148-154.
[15] Laird NM and Ware JH. Random-effects models for longitudinal data. Biometrics 1982; 38: 963-974.
[16] Collins JA, Schandi CA, Young KK, Vesely J and Willingham MC. Major DNA fragmentation is a late event in apoptosis. J Histochem Cytochem 1997; 45: 923-934.
[17] Fresno Vara JA, Casado E, de Castro J, Cejas P, Belda-Iniesta C and Gonzalez-Baron M. PI3K/Akt signalling pathway and cancer. Cancer Treat Rev 2004; 30: 193-204.
[18] van der Luit AH, Vink SR, Klarenbeek JB, Perrissoud D, Solary E, Verheij M and van Blitterswijk WJ. A new class of anticancer alkylphospholipids uses lipid rafts as membrane gateways to induce apoptosis in lymphoma cells. Mol Cancer Ther 2007; 6: 2337-2345.
[19] Pantelouris EM. Absence of thymus in a mouse mutant. Nature 1968; 217: 370-371.
[20] Lingwood D and Simons K. Lipid rafts as a membrane-organizing principle. Science 2010; 327: 46-50.
[21] Daleke DL. Phospholipid flippases. J Biol Chem 2007; 282: 821-825.
[22] Chen R, Brady E and McIntyre TM. Human TMEM30a promotes uptake of antitumor and bioactive choline phospholipids into mammalian cells. J Immunol 2011; 186: 3215-3225.
[23] Cho DC. Targeting the PI3K/Akt/mTOR Pathway in Malignancy: Rationale and Clinical Outlook. BioDrugs 2014; 28: 373-81.
[24] Opel D, Poremba C, Simon T, Debatin KM and Fulda S. Activation of Akt predicts poor outcome in neuroblastoma. Cancer Res 2007; 67: 735-745.
[25] Li Z and Thiele CJ. Targeting Akt to increase the sensitivity of neuroblastoma to chemotherapy: lessons learned from the brain-derived neurotrophic factor/TrkB signal transduction pathway. Expert Opin Ther Targets 2007; 11: 1611-1621.
[26] Li Z, Tan F, Liewehr DJ, Steinberg SM and Thiele CJ. In vitro and in vivo inhibition of neuroblastoma tumor cell growth by AKT inhibitor perifosine. J Natl Cancer Inst 2010; 102: 758-770.
[27] Brodeur GM. Getting into the AKT. J Natl Cancer Inst 2010; 102: 747-749.
[28] Fulda S. The PI3K/Akt/mTOR pathway as therapeutic target in neuroblastoma. Curr Cancer Drug Targets 2009; 9: 729-737.
[29] Ruiter GA, Zerp SF, Bartelink H, van Blitterswijk WJ and Verheij M. Alkyl-lysophospholipids activate the SAPK/JNK pathway and enhance radi-

ation-induced apoptosis. Cancer Res 1999; 59: 2457-2463.
[30] Verma G and Datta M. The critical role of JNK in the ER-mitochondrial crosstalk during apoptotic cell death. J Cell Physiol 2012; 227: 1791-1795.
[31] Melzer HI, Coppenrath E, Schmid I, Albert MH, von Schweinitz D, Tudball C, Bartenstein P and Pfluger T. (1)(2)(3)I-MIBG scintigraphy/SPECT versus (1)(8)F-FDG PET in paediatric neuroblastoma. Eur J Nucl Med Mol Imaging 2011; 38: 1648-1658.
[32] Weichert JP, Pazoles C. Personal Communication 2013.
[33] Becher OJ, Trippett TM, Kolesar J, Gilheeney S, Jiang Z, Khakoo Y, Lyden D, Sima C, Holland EC and Dunkel IJ. Phase I study of single-agent perifosine for recurrent pediatric solid tumors. ASCO Meeting Abstracts 2010; 28: 9540.
[34] Pachioni Jde A, Magalhaes JG, Lima EJ, Bueno Lde M, Barbosa JF, de Sa MM and Rangel-Yagui CO. Alkylphospholipids - a promising class of chemotherapeutic agents with a broad pharmacological spectrum. J Pharm Pharm Sci 2013; 16: 742-759.
[35] Bagley RG, Kurtzberg L, Rouleau C, Yao M and Teicher BA. Erufosine, an alkylphosphocholine, with differential toxicity to human cancer cells and bone marrow cells. Cancer Chemother Pharmacol 2011; 68: 1537-1546.
[36] Kotting J, Marschner NW, Neumuller W, Unger C and Eibl H. Hexadecylphosphocholine and octadecyl-methyl-glycero-3-phosphocholine: a comparison of hemolytic activity, serum binding and tissue distribution. Prog Exp Tumor Res 1992; 34: 131-142.
[37] Verweij J, Krzemieniecki K, Kok T, Poveda A, van Pottelsberghe C, van Glabbeke M and Mouridsen H. Phase II study of miltefosine (hexadecylphosphocholine) in advanced soft tissue sarcomas of the adult--an EORTC Soft Tissue and Bone Sarcoma Group Study. Eur J Cancer 1993; 29A: 208-209.